Fire Safety Journal 163 (2026) 104857

Contents lists available at ScienceDirect

Fire Safety Journal

journal homepage: www.elsevier.com/locate/firesaf

Crib-fire dynamics in open and enclosed ventilation conditions

Alexander L. Brown [a,*], Sara McAllister [b], Alexander J. Josephson [c], Jon Reisner [c], Eunmo Koo [c]

[a] Sandia National Laboratories, PO Box 5800, Albuquerque, NM, USA
[b] United States Forest Service, 5775 US Highway 10, Missoula, MT, USA
[c] Los Alamos National Lab, PO Box 1663, Los Alamos, NM, USA

ARTICLE INFO

Keywords:
Compartmentalization
CFD
Crib fires
Modeling

ABSTRACT

Crib fires are a way to produce fires with higher repeatability than generally is the case for wildland and urban scenarios and consequently are used to study fire behavior. Models for simulating large-scale fires benefit from characterization against relevant test conditions. Here we describe a modeling and experimental effort to better explore fire dynamics at the larger range of what is achievable in laboratories. The modeling that corresponds to the tests is used to provide parameters to larger-scale transport modeling efforts for climate effects as well as to evaluate modeling under oxygen vitiated conditions arising from partial enclosure conditions. Modeled pyrolysis rates and environmental conditions correspond reasonably well to the extinction regimes articulated in prior experimental work for under-ventilated fires expressed via the ventilation parameter for five ventilation conditions that vary across different response regimes. This suggests several potential aspects of model utility for large urban scenarios where structures restrict ventilation, and fires burn differently in response to the change in oxygen availability.

1. Introduction

The study of fires is often complicated by the variable nature of fuel sources. In this work, we are focused mostly on solid fuels, as liquid and gas fuels have specific handling processes affiliated with them due to their mostly designed function as a fuel. Solid fuels in fires are often not intended to be fuels (wood in campfires, coal power, prescribed wildland burns, and charcoal for grilling being some noted exceptions here). At the highest level of classification there are urban and wildland fires that garner the focus of assessment studies. Urban fuels fall into three main categories: residential, industrial, and commercial; with these sometimes further broken down into sub-categories such as commercial-retail or commercial-office. Wildland fuels vary according to biome, land usage or management, fire history, and season. Regardless of the classification, there can be large fuel variability in mass, volume, arrangement and type that make fire assessments challenging. Fuel loadings depend on the use cases and can vary significantly on yearly, monthly, daily, or even hourly basis. Since fires are typically unplanned events, fuels are often poorly characterized at the time of the fire and have a high uncertainty in post-fire assessments. This presents a challenge for the fire modeling and assessment communities.

To enhance the ability to characterize fire behavior, it is desirable to have a more regular definition of a fire for laboratory testing. Crib fires are constructed arrays of regular solid fuels that exhibit a much higher degree of repeatability than most fuel sources in fires of concern. Consider the complexity of a tree or a shrub geometry or chemistry in the context of a wildland application. Or consider an urban residential fire, where furniture and household goods may be the prime contributors to the fire. A crib can reduce the variability of the fuel source and allow for improved interrogation of other parts of a fire under conditions more amenable to replication. Crib fires have been widely studied since they provide fire scientists with informative results that exhibit a degree of repeatability that is not otherwise readily possible using unprocessed biomass. The first crib tests are alleged to have been conducted by Folk in 1937, although this may be only the first documented tests of this nature and not necessarily the first crib fire (see Smith and Thomas [1]). More recently, there have been many who have leveraged the concept for fire studies (e.g., Refs. [2–12]), including a recent review [9] and a report specifically targeting large-scale fires [11].

Recently, crib fires have been the subject of simulation activities

This article is part of a special issue entitled: FISJ_IAFSS 2026 published in Fire Safety Journal.

* Corresponding author.

E-mail addresses: albrown@sandia.gov (A.L. Brown), sara.mcallister@usda.gov (S. McAllister), alexanderj@lanl.gov (A.J. Josephson), reisner@lanl.gov (J. Reisner), koo_e@lanl.gov (E. Koo).

https://doi.org/10.1016/j.firesaf.2026.104857
Received 24 September 2025; Received in revised form 8 April 2026; Accepted 21 April 2026
Available online 2 May 2026

using computational fluid dynamics (CFD) models. Most CFD codes deal with fluid flow using Eulerian frameworks and the Navier-Stokes equations. Fewer codes can simulate heat transport and reactions, which require additional physics including energy and species equations. Even fewer codes can simulate reacting solids and fires. This necessitates models for the burning of materials initially in the solid state but often transition to a fluid state during a series of complex reactions. This level of complexity for physics models is rare in CFD codes not specifically designed for this purpose. For this reason, there are few instances of reports in the open literature using codes where crib fires have been predicted using CFD models. Most widely reported in the literature are simulations using the Fire Dynamics Simulator (FDS), including [13–15]. In these studies, the methods for approximating the crib behavior are either based on cone calorimeter or prescribed heat release rates or a 1-step Arrhenius reaction, and scenarios are simulated with the intent to show predictivity. Most of these involve some degree of calibration, and pyrolysis reactions are not explicitly resolved on fully representative solid wood geometry. Mesh refinement is done with coarse scenarios insufficiently resolved to represent the identical and consistent geometry of the corresponding experiments.

Another CFD modeling option, used here, is SIERRA/Fuego. SIERRA is an architecture for computational engineering simulations that is developed and maintained by Sandia National Labs [16]. It provides generalized solvers, data structures, and tools for the computational physics necessary to simulate a wide variety of engineering computational problems. The Fuego sub-unit is one of the Thermal/Fluid sub-mechanics tools. Fuego is a fire simulation sub-unit, which is designed with many of the elements needed to predict the consequences of an abnormal thermal event. SIERRA/Fuego development was originally driven mainly by the need to predict the thermal response of cargo to transportation fires. The development was focused on the heat transfer to an object inside the fire and was focused on length-scales consistent with transportation packages (meters to tens of meters). However, SIERRA/Fuego has also been characterized for simulating intermediate-scale (tens to thousands of meters) problems that are outside the typical scale of the nominal case scenarios that were the target of the initial development of the code. Because the SIERRA tools are targeted for the large high performance compute clusters, it made sense to leverage this resource and attempt higher-resolution predictions that matched the test geometry. Furthermore, the effort provided an opportunity to leverage a higher fidelity representation of the crib via direct pyrolysis reaction kinectics compared to the historical approaches that circumvented this aspect of modeling to accommodate under-resolved geometry.

More recently, the prediction capabilities have been extended to simulate trees and forests on fire [17,18]. The Lagrangian particle model is used to simulate wildland fuels with a random dispersion of reactive particles of varying size. These particles behave like fuel, and pyrolyze and burn in response to heating. These methods are a reasonably approximate way to simulate wildland fire behaviors and were shown in both studies to produce reasonably representative burn results in terms of mass loss, burn duration, and rate of propagation for at least some of the scenarios of interest. The Lagrangian methods are well-suited to wildland scenarios because they are able to represent the fuel through statistical distributions, which is characteristic of the actual fuel. Limitations include the lack of conductive heat transfer for the dispersed fuel particles, the misrepresentation of the fluid drag over the simplified spherical fuels compared to real fuels, and the under-resolved sub-grid behaviors of the fuels and fires that are occurring in the actual samples when compared to the simulations.

Laboratory wood-crib fires are of high interest to creating simulations of large-scale urban or wildland fire phenomenology as they serve as highly repeatable "unit tests" for fire-model physics (e.g., Ref. [19]): their well-characterized geometry and heat-release profiles let researchers pin down combustion, emission, radiation, and buoyant-plume parameters in CFD codes before those same codes are unleashed on far more complex, high-consequence scenarios. After a model can reproduce the burning-rate and thermal field of a single or arrayed crib, its sub-grid algorithms are transplanted into landscape-scale fire simulations. Some examples include Albini's large-fuel burnout model, which was tuned with crib-burn data to predict coarse-woody-fuel consumption during wildland mega-fires [20], and Ene's FDS calibration Model for office fires, where full-scale room tests with nine cribs were used to calibrate Fire Dynamics Simulator (FDS) predictions of travelling-fire spread across open-plan offices [21]. In this way, the crib fire acts as an empirical bridge, allowing confidence-tested heat generation, fuel consumption, and smoke-plume physics to propagate upward from bench scale to the kilometer-scale numerical domains required for forecasting modern mega-fires in both wildland and urban settings. The discussion section of this work, will demonstrate such a potential empirical bridge from the soot production and lofting potential results of this work to large-scale urban fire modeling.

This current work is a multi-faceted approach to the crib fire scenarios using SIERRA/Fuego and laboratory testing on the larger-scale side of the problem space. One novelty factor is that a different code other than FDS is being used to simulate the scenarios. This comes with a different physics model and approach. An effort is made to characterize the predictions to a recent dataset obtained from the USDA laboratories in Missoula, Montana, USA. A final facet to the problem is the extension of the open crib fire scenario to a scenario more representative of urban conditions. A partial enclosure with a variably sized opening is used to explore the ability of the predictions to replicate expected behaviors using the extinction parameter as derived from historical enclosure fire scenario assessments. The objectives of this work include developing methods for simulating crib fires, characterizing the accuracy of the methods by comparisons to data, exploration of the predicted variability in emissions and fire behaviors for predicted compartment fires with an emphasis on the ventilation parameter and extending the work to larger-scale applications.

2. Methods

2.1. Experimental

Two large wood crib experiments were conducted in the burn chamber of the Missoula Fire Lab. The cribs were built with 2.5 cm square cross-section ponderosa pine dowels that were 1.22 m long (see Fig. 1 (left)). These were arranged in evenly spaced cross-piles with 9 sticks per layer and 24 layers (spacing between sticks was 12.4 cm). Small finishing nails were used to hold the crib together. The crib was placed on a 1.8 m square platform of mineral fiber board (replaced after each test). In the first test, the platform was also covered with multiple sheets of ceramic paper insulation. Fire bricks at the corners of the crib kept it 12.7 cm above the platform to allow for air to flow underneath and up through the crib [9,22] that actively weighed the contents during the course of the test at 100 Hz. While the wind boundary conditions were not specifically controlled, the test was conducted inside a largely quiescent burn chamber with dimensions of 12 m $\times$ 12 m x 20 m, much larger than the crib itself. Because of the spacing of the dowels, the crib is relatively low-density in terms of the fuel, with the wood fuel composing about 20% of the volume of the crib. In terms of crib metrics, the porosity of the crib was $\phi = 0.22$, well into the loosely packed regime [4].

To assure ready ignition, about 1.5 L of 99% isopropyl alcohol was sprayed over the wood crib before ignition to provide the heat necessary to ignite the solid fuels. A small amount of fuel dripped off the crib onto the ceramic paper and mineral board below, where it burned briefly as a pool fire. To ensure a faster ignition of the center, an additional 1.0 L of alcohol was poured into a 2.5 cm deep, 30.5 cm diameter pan and placed under the crib. Though some alcohol in the pan remained burning for about 90 s into the test, the alcohol used for ignition was observed to

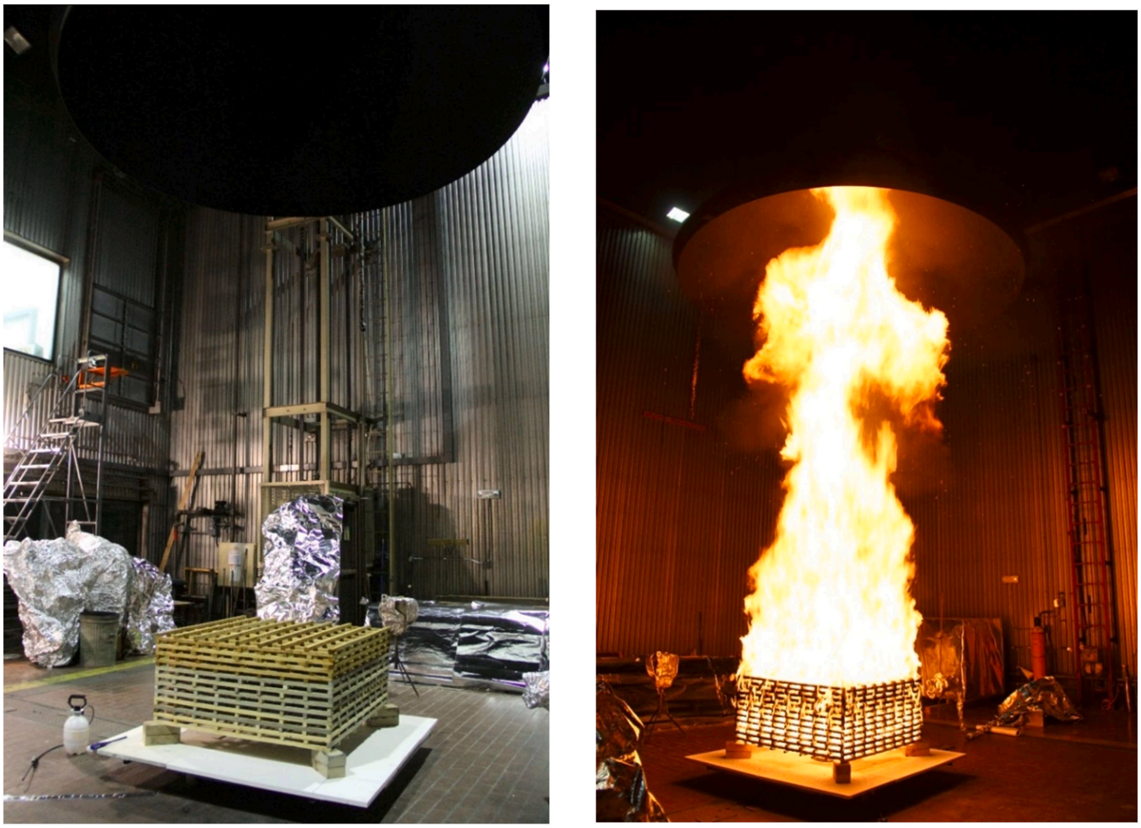

Fig. 1. Left: A photograph of the crib fire test prior to ignition. Right: An image of the steady burning achieved during the second test, showing the flame reaching up into the ventilation hood 6 m above.

largely burn off early in the experiment duration, before the steady state burning of the wood was achieved. For the first experiment, the wood was room-conditioned with approximately a 6% moisture content. For the second experiment, the wood was placed in a conditioning chamber for over two weeks before the experiment at 35 °C and 3% RH for an equilibrium moisture content of about 1%. The steady burning rate, defined here as the mass loss rate, was found using a simple linear regression of the mass loss data over a period of 80 s.

The resulting fire was at full-scale producing very high flames (over 6 m) with the interior of the crib well engulfed in flames as suggested by Fig. 1 (right).

2.2. Modeling

2.2.1. Simulation software

Computational fluid dynamics (CFD) simulations from SIERRA/Fuego are used to model the crib fire and explore the predicted variability in emissions and fire behaviors for compartment fires with different ventilation parameters. SIERRA is developed at Sandia, and selection of this tool was therefore convenient for the project. Navier-Stokes solvers predict the flow through momentum and continuity equations. Enthalpy and species equations are solved for thermal reactions. Various treatments of turbulence are available, with this work performed with the Temporally Filtered Navier Stokes (TFNS) model [23], featuring hybridization of large-eddy simulation and k-ε model capabilities. Several reaction models exist, and this work leverages the eddy dissipation concept (EDC) model [24,25], which is a mixing-limited approximation for under-resolved flaming combustion in CFD simulations. Radiative heat transport is solved via a discrete ordinates solver, in this case linking to the solver in the Nalu sub-module. Soot is modeled via a two transport equation method (soot mass fraction and soot nuclei number) with source terms based on the work of Tesner et al. [26]. Version 5.9.4 of SIERRA/Fuego was used for the simulations described herein, and the verification testing includes nightly regression tests, as well as a more dedicated campaign to demonstrate coding adequacy through methods of manufactured solution (MMS) and unit testing. Validation includes 25+ years of model comparisons to data, with significantly more detail available in the manuals.

2.2.2. Domain definition and ignition

The crib as tested was assumed nominal in size, and the 2.5 cm square dowels were arranged according to the test description in the Cubit geometry engine. The solid material was subtracted from a domain mesh, which had the fuel pan and the floor beneath. To simplify the ignition protocol, the fuel pan was assumed to be 1.45 m square. A small geometry encompassing the crib and pan was initially provided to the meshing software, with any needed extensions of the geometry in height or width to be produced later by extending the mesh at the boundaries.

An image of the baseline crib geometry is found in Fig. 2. The wood is purple, the fuel pan blue, and the wall boundary conditions here are green.

The enclosed domain was 3.04 m high, and 5 m square with the crib in the middle of the room. The meshing tool reports the flow volume as 74.4 m^3, with the recessed pan adding to the volume and the wood subtracting from the volume that would otherwise be 76 m^3 based on the nominal room dimensions. The room size was selected to be representative of office or residential spaces, and also to provide sufficient volume such that the fire did not dominate the domain.

The ignition of the liquid fuel is simulated as if it had all collected in the pan beneath the crib, neglecting the potential for absorption from the test preparation in the experiments such that all the liquid fuel evaporated from the pool. The pool fire was ignited, which in turn

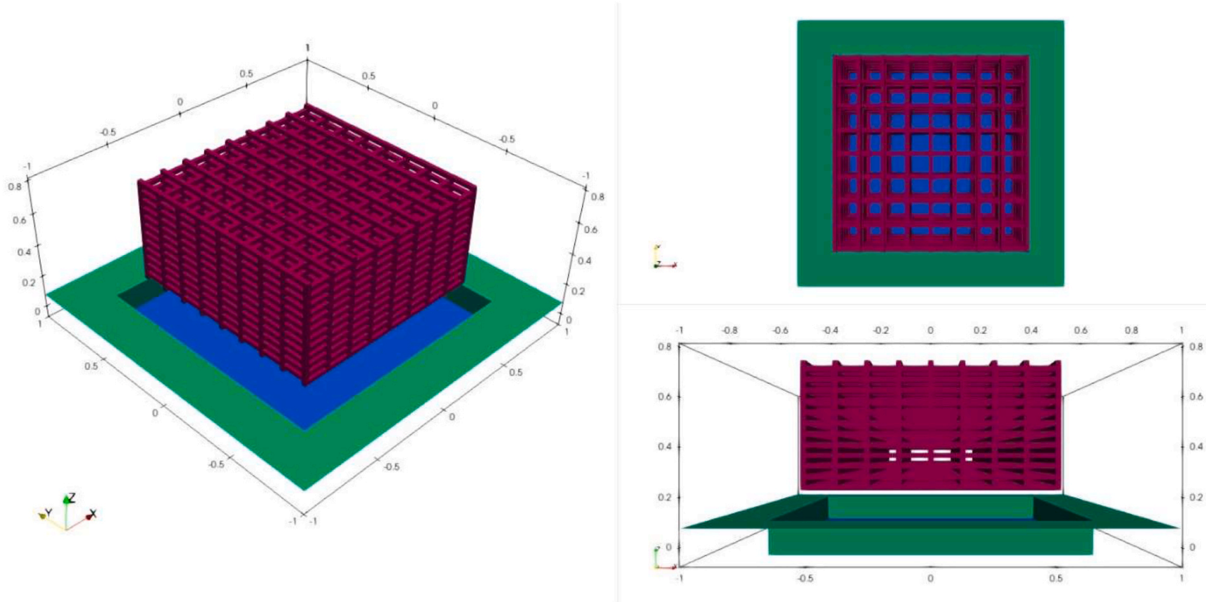

Fig. 2. An illustration of the base geometry with dimensions marked in units of meters. A top view is shown in the upper-right, a side view in the lower right, and an isometric view in the left.

ignited the wood once it had heated to the point where it was pyrolyzing. The pool model in Fuego was used that approximates the liquid as a 1D layer of liquid that evaporates in response to the enthalpy input from the flames. This resulted in a full steady burn of the fuel over about 40-50 s under open conditions, after which burnout began to limit the intensity of the burn over the next 40 s or so with the pool ceasing to contribute flames around the same time as was observed in the tests at about 90 s.

The wood was modeled with a 1D boundary condition that assumes each face is 1 cm deep with 8 intervals 1.25 mm thick each. A conduction equation was solved for each layer, with the pyrolysis of the wood producing 30% char, 20% water, and 50% fuel. The gas-phase fuel assumed was a surrogate C_8H_{18}, which was selected for convenience. The pyrolysis yielded extra water to achieve a net heating value of the burning fuel to be approximately that of burning wood (about 20 MJ/kg) which also helps keep the elemental distribution of products similar to that of wood. Since our version of the EDC model only permits a single hydrocarbon fuel, the liquid fuel in the pan was also simulated with the same (30% water diluted to simulate alcohol heat of combustion) surrogate fuel. A single step Arrhenius pyrolysis reaction was used ($A = 1.43 \times 10^7\ s^{-1}$, $Ea = 88.61$ J/molK). A low conductivity (1 W/mK) and typical density (600 kg/m^3) for wood [17] were assumed. A 1D fuel regression model was used to simulate the pool burn.

The enclosure walls were also simulated as a 1D non-reacting solid wall medium with density of 1600 kg/m^3, specific heat of 600 J/kgK, and thermal conductivity of 0.2 W/mK. They were 1 cm thick, with four nodes, and each node was 2.5 mm thick, with an adiabatic backside condition. This provided a feedback mechanism to account for the heat-up of the structure and its effect on the thermal conditions in the domain.

2.2.3. Meshes and open boundaries

There were several meshes created based on the baseline geometry described above. The coarse mesh resolution was set to the thickness of each dowel (2.5 cm). 2:1 refinement and greater meshes were also generated, although these simulations took significantly longer to perform. Mean centerline temperature profiles were compared for the nominal case with the refined predictions to demonstrate adequate resolution for the nominal mesh scenario. We found mass change of the crib and temperature at 1 m elevation to be sufficiently similar between the two out to 30 s to continue with the coarser mesh for the full study. Corresponding plots are included in the supplemental material. Furthermore, a more detailed validation study of mesh resolution for a 1-m buoyant plume at this range of resolution is found in Refs. [27,28], illustrating respectable convergence of mean and fluctuating velocities at this nominal resolution. For the open fire scenarios, the final height and width of the geometry was much greater than that illustrated in Fig. 3F. These were open parameters, which were progressively increased to achieve the needed goals of the various phases of testing. Preliminary simulations were performed with a mesh that had a 2.5 m square cross-section, and was just over 7 m high.

The preliminary phase involved modeling with multiple meshes to ensure the final mesh used produces acceptably approximate results as the finer mesh. It also involved tuning the heat of pyrolysis to give the approximately 0.3 kg/s steady-state pyrolysis rate as obtained in the experimental tests (see Results below). Since the simulation methods did not involve water evaporation and the moisture of the cribs was low (1-5%), it is assumed that the effect of the evaporation could be lumped in with the pyrolysis endotherm and still achieve a representative fire (see below).

The next phase of modeling involved locating the crib in the middle of a 5 m square room that was 3.04 m tall. The same basic crib-centric mesh was used, and a gradually expanding mesh was applied to extend the domain out to the full extent. The boundary conditions for the room were wall boundaries, with the exception of the floor, the pan, and a door or window open boundary at the center of one of the four faces of the room. Table 1 gives nominal dimensions for the open boundary.

Because mesh conformal application of the boundary conditions was used, the height and width of the doors did not exactly match the nominal dimensions for the openings. Table 2 shows actual dimensions, which are a minor departure from the intended nominal dimensions. Case F is the open burn scenario (approximating experimental conditions), which has semi-infinite opening as the open boundary condition was on five of the six sides of the rectangular mesh.

Illustrations of the coarse version of these meshes are found in Fig. 3. This arrangement of the scenarios will be used consistently in subsequent plots to illustrate planar contour plot results of various predictions from the simulations.

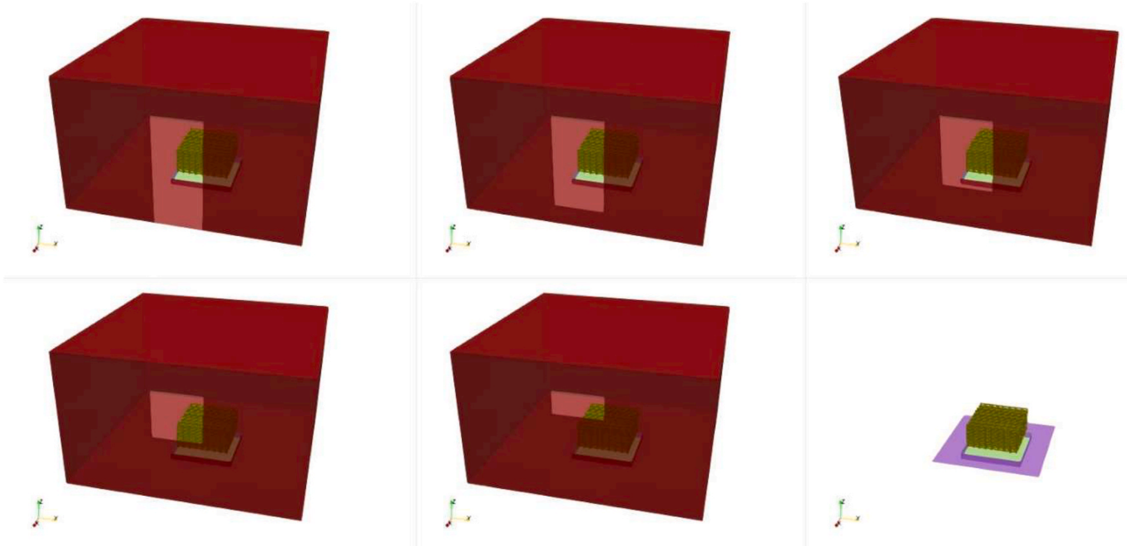

Fig. 3. An illustration of the various geometries for the simulations, including left to right then top to bottom for cases E, D, C, B, A, and F.

Table 1
Nominal open boundary dimensions.

Case	Opening Width (m)	Opening Height (m)
A	1	0.5
B	1	1
C	1	1.5
D	1	2
E	1	2.5

Table 2
Actual open boundary dimensions.

Case	Opening Width (m)	Opening Height (m)	Area (m^2)
A	1.02015	0.478052	0.487685
B	1.02015	0.983412	1.003228
C	1.02015	1.48877	1.518769
D	1.02015	1.97045	2.010155
E	1.02015	2.40225	2.450655
F	NA	NA	NA

2.2.4. *Enclosure scenarios*

A lack of ventilation in a partially-ventilated chamber will inhibit oxygen replenishment and eventually extinguish burning media. With the enclosure meshes and a physical model for a crib fire, it should be possible to assess whether the simulations are able to predict extinction due to the lack of ventilation. This helps demonstrate the accuracy of the tools predicting the heating feedback mechanism between the fuel and the flames. Historical work on enclosure fires has developed the notion of an extinction or ventilation parameter defined as:

$$\Theta = \rho g^{1/2} A_o (H_o)^{1/2} / A_F \quad (1)$$

which is a parameter-based method for assessing the steady-state burn rate based on the opening size. Here Θ is the ventilation parameter (g/m^2-s), ρ is gas density (g/m^3), g is the acceleration of gravity (m/s^2), A_o is the exhaust opening area (m^2), H_o is the height of the opening (m), and A_F is the area of fuel on fire (m^2). Following the nomenclature and theory of Utiskul et al. [29] and the findings of Torero et al. [30], when the extinction parameter is below about 2000 (g/m^2-s) there is a decrease from free burn conditions, and below 1000 (g/m^2-s) there tends to be flame extinction. Consequently, the enclosure simulations included varied openings ranging from door-sized (6700 g/m^2-s) to a small window-sized (600 g/m^2-s), which spans the range of ventilation parameters from open burning to extinction as characterized from the contributing datasets. Based on the Utiskul et al. [29] study, extinction Zone 1 has a ventilation parameter below 200 g/m^2-s, the transition to the next higher phase is at about 1000 g/m^2-s. At 2000 g/m^2-s and above, the fire behaves as a free burn, albeit slowed by the ventilation restriction.

2.2.5. *Open scenario characterization*

The model employed did not include a moisture evaporation step, lacking accurate test data and a validated model therefore. Instead, an adjustment was made to the heat of pyrolysis to account for the solid fuels' moisture evaporating (estimated at 5% moisture content) and to achieve matching burn rates to the tests. Because there is significant uncertainty in the heat of pyrolysis, this was used as a single tuning parameter. The rate of mass loss of the crib at steady-state was known from the experiments to be about 0.3 kg/s (as per Fig. 5). Anticipating the heat of reaction to be endothermic about 1×10^3 kJ/kg based on the work of Antal et al. [31], it was not surprising to find the heat of reaction that best replicated the burn rate to be a bit higher at about 1.35×10^3 kJ/kg, as seen in Fig. 4. This parameter captures both the main effect of heat of reaction of the wood, as well as more minor effects

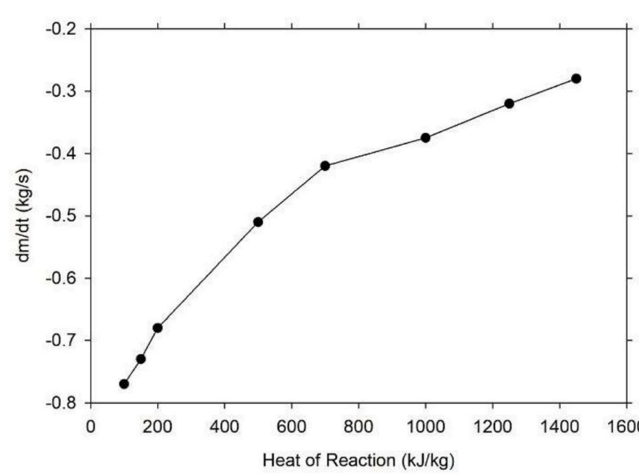

Fig. 4. Steady-state crib burn rate as a function of simulated heat of reaction of the wood.

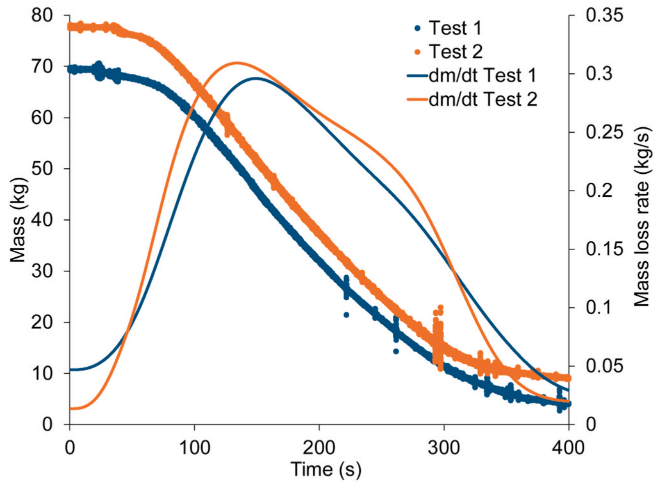

Fig. 5. Experimental mass (left axis) and mass loss rate (right axis) of two large wood cribs.

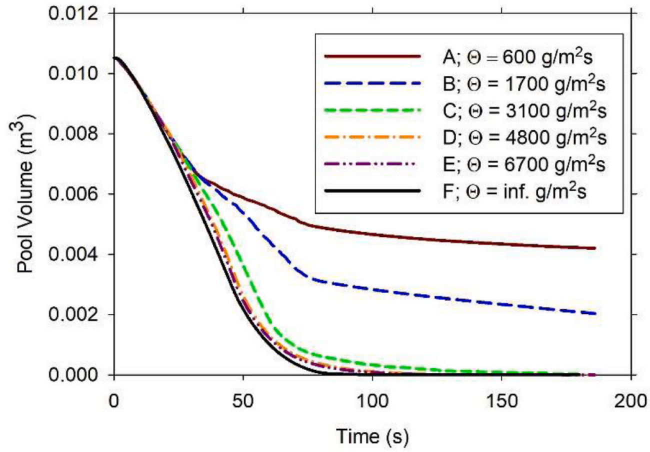

Fig. 6. Predicted pool fuel volume showing the evaporation of the liquid used to ignite the crib fire with the ventilation parameter indicated in the legend.

from fuel moisture evaporation. Subsequent simulations are all performed with this as the model parameter accounting for both evaporation and pyrolysis heating in a single parameter.

Heat of reaction significantly affects the steady-state mass loss rate. For applications without test data like this one, the parameter will need to be accurately determined either through direct measurements or calibration, and validation can help establish the propriety of the model along with selected parameters.

3. Results

3.1. Testing

Testing results at the USFS facility provided the basis for the open crib model work (case F). Fig. 5 compares the measured mass loss and mass loss rates of the two cribs. Note that the mass of the weighing platform, support bricks, and metal pan have been subtracted out. The continuous mass loss rate was found by taking the numerical derivative of the spline fit of the mass data with ten degrees of freedom. The mineral fiber board was reweighed after each test and was found to have lost 0.9 kg in the first test and 2.3 kg in the second test; however, this constitutes at most 3% of the crib mass and is thus not considered to have a large impact on the overall burning rate. The peak burning rate was 0.30 kg/s for the first test and 0.31 kg/s for the second test. Using a linear regression, the average burning rates between 110 and 190 s after ignition were 0.29 kg/s for the first test and 0.30 kg/s for the second test. As noted earlier and indicated in Fig. 1, the steady flame heights were easily over 6 m during the tests in both cases. The mass was recorded for 30-45 min after ignition (not shown) until all remaining visible flames were extinguished and glowing mostly subsided. The cribs were observed to begin collapsing at 200-250 s after ignition, with large collapsing events reflected as noise in the mass data. The final weight after the crib collapsed and the remaining char is consumed reflects both the mass loss in the fiber board and material that dropped off the platform as the cribs collapsed.

3.2. Simulations

Each pool fire in all simulations was ignited under similar circumstances as the experiments. There was plenty of oxygen in the room initialized as ambient air, and the liquid pool fire ignited and began to heat the wood above it. This is seen in Fig. 6, where all the scenarios trend together initially. By about 30 s, the effect of the enclosure starts to manifest, and the liquid fuel evaporation slows for scenarios where the oxygen is more limited. The case with the smallest opening, case A, exhibits only about half of the pool volume evaporating and fits the ghosting/oscillation regime ($\Theta < 1000$ g/m^2-s), where historical testing suggests variable response including the potential for extinction and localized flaming near the opening [29]. Case B fits the oscillation regime below free burn ($\Theta < 2000$ g/m^2-s), a transitional regime exhibiting restricted burning.

Simulation results illustrate a significant reduction in burn rate depending on size of the openings as indicated by the crib mass loss as a function of time in Fig. 7 A. Correspondingly in Fig. 7 B, the soot exhaust rate is low for low Θ scenarios (600 and 1700 g/m^{2}s) with poor ventilation. For intermediate and higher ventilation scenarios, the soot exhaust is not linear, with the 3100 g/(m^{2}s) scenario yielding the most soot even though the mass loss is lower, sustaining a longer emission at the higher rate. These scenarios did not allow for oxidation outside the room, which may further reduce the soot emissions into the environment for intermediate Θ scenarios depending on whether or not there are flames outside the opening. In the longer-term, the scenarios with increased ventilation are expected to yield more soot to the environment since they result in increased burning and a faster burn rate of the solid.

At 180 s, a series of center-plane temperatures as shown in Fig. 8 illustrate the effect of the opening on the environment temperature. In all cases, the temperatures in the enclosure are elevated compared to the open case. In case A with the least ventilation (middle bottom frame), the temperatures are the lowest, with the hottest found in case E (top left) where the walls provide thermal feedback to the fire, and the burn is active. This is best illustrated through similar plots of the oxygen mass fraction, as found in Fig. 9. The cases with increased ventilation have more oxygen present in the enclosure, allowing for increased heat release of the pyrolysis products from the crib via combustion.

Fig. 10 shows instantaneous soot mass fraction predictions at a similar 180 s time. The open burning scenario (bottom right) suggests more soot, but with active burning above the crib and a higher net burn rate (see Fig. 7), the soot emissions are not necessarily significantly higher. This is because soot is a dynamic parameter functionally affected by the oxidation mechanism that is environmentally dependent and not necessarily a direct function of the quantity of fuel burnt. The enclosed scenarios show lower soot with less ventilation. The soot is more concentrated in cases D and E (top middle and left), whereas it is more evenly spread around the room in case C (top right), likely due to improved burn-out conditions in cases D and E compared to case C.

Further assessment of the compartment simulation behavior is found in Fig. 11, where average temperatures are similar for the first 20-30 s, after which the effects of ventilation start to result in lower mean compartment temperatures for scenarios with less ventilation. The fraction of total enthalpy contributing to wall heating is shown (time

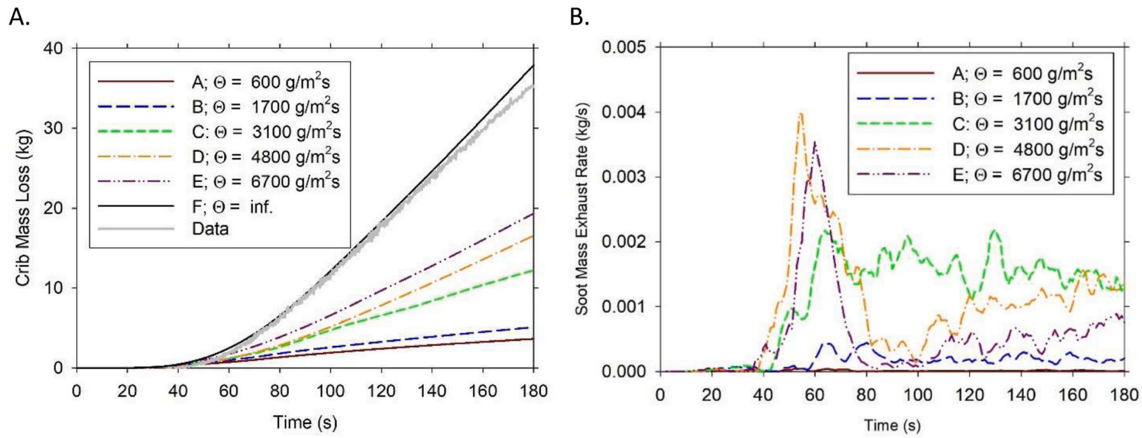

Fig. 7. Predicted crib mass loss and soot mass exhaust rate for different ventilation parameter (Θ) scenarios.

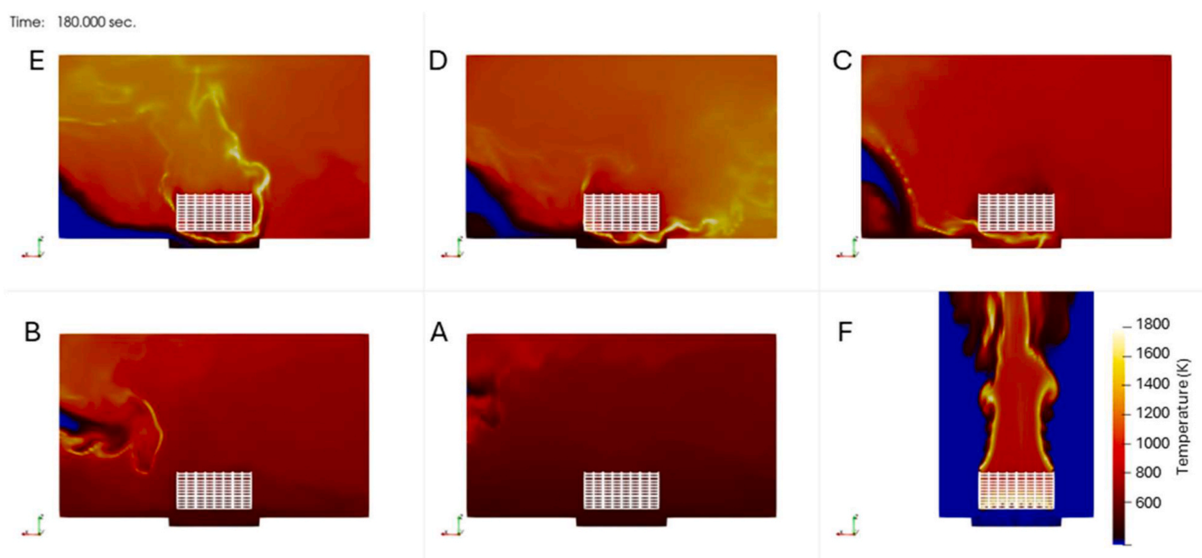

Fig. 8. Predicted center-plane gas temperatures at 180 s for the six simulation cases with varying ventilation.

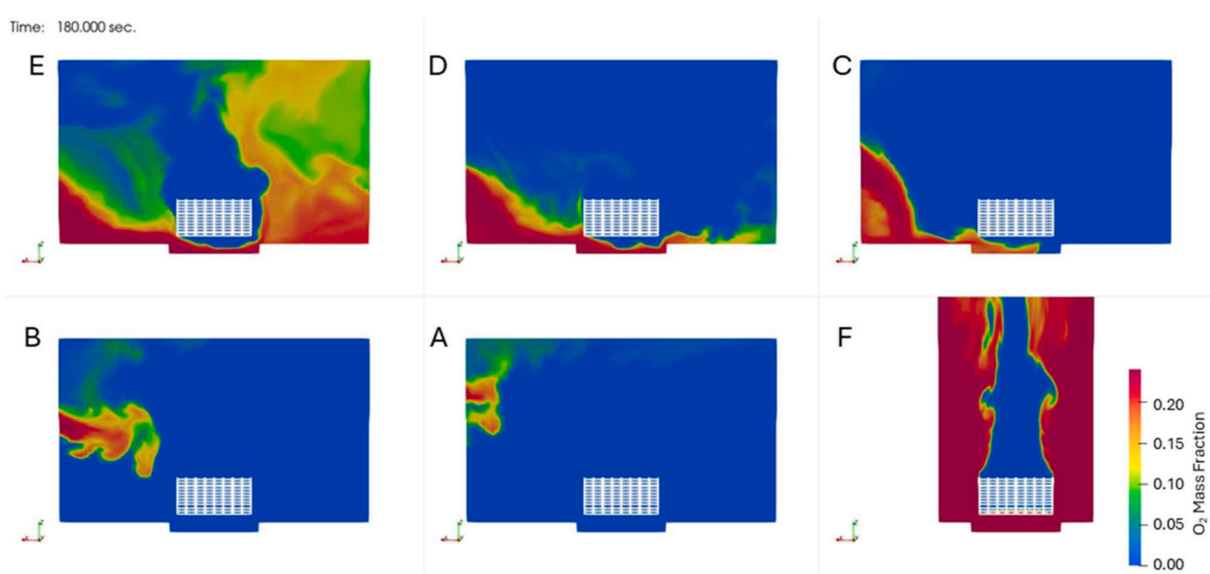

Fig. 9. Predicted center-plane oxygen mass fraction at 180 s for the six simulation cases with varying ventilation.

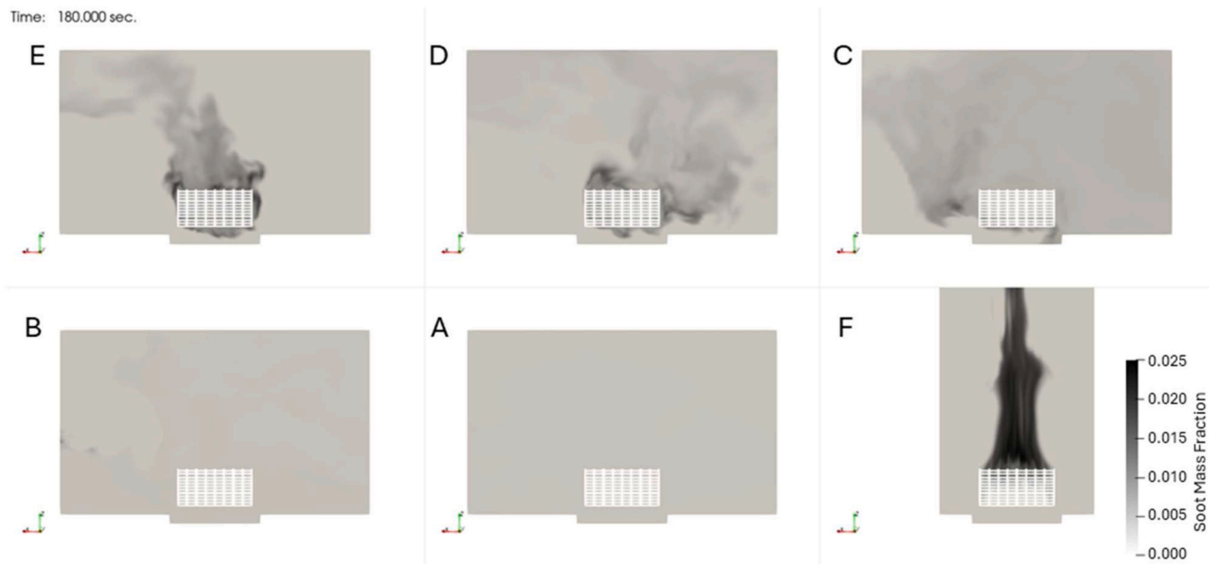

Fig. 10. Predicted soot mass fraction at 180 s for the six simulation cases with varying ventilation.

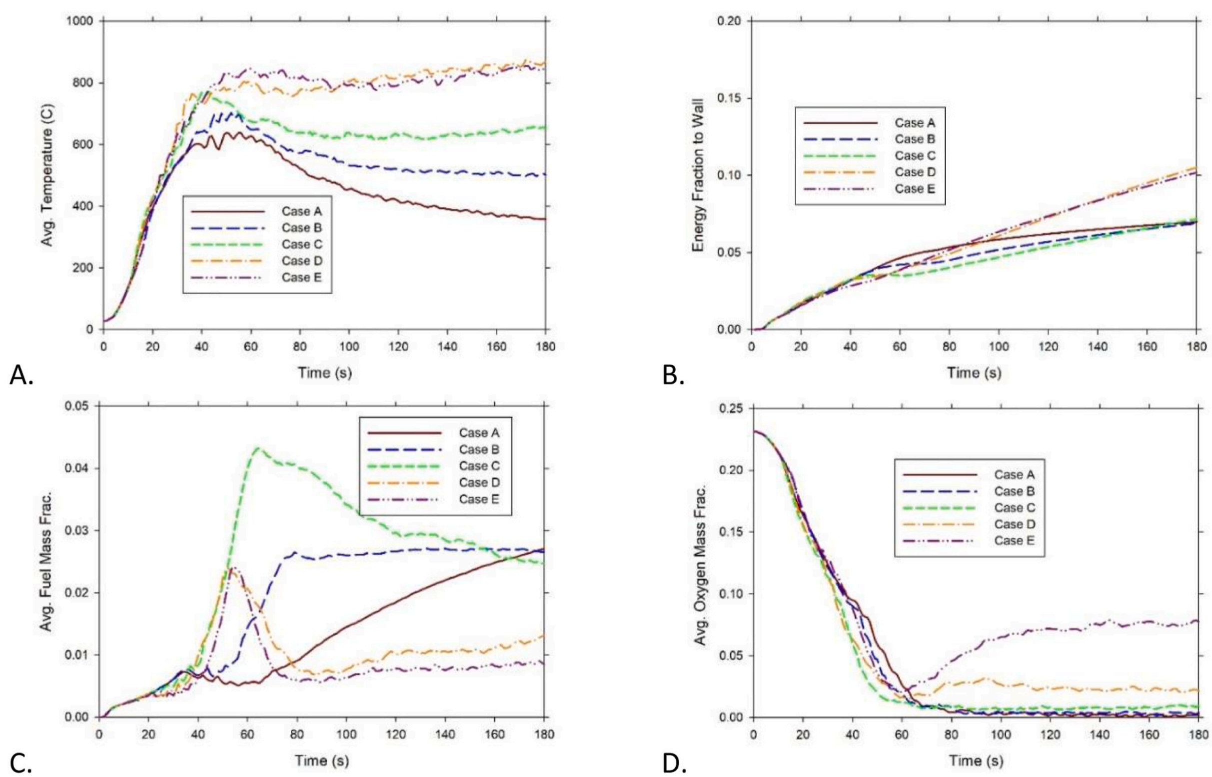

Fig. 11. Volume integrated parameters and wall enthalpy fraction of total HRR for enclosure scenarios.

cumulative), with the fraction increasing with time, and a larger fraction at later times for the scenarios with improved ventilation. Over 10% of the heat from the fire goes to heating the walls for the ventilated cases, with the fraction trending upwards at 3 min.

Mean oxygen and gaseous fuel in the volume are shown as a function of time (Fig. 11C and D). Scenarios are relatively similar in this respect for the first 60 s, after which the better ventilated cases diverge from the downward trend and can establish an inflow and replenish the oxygen thereafter. Modeled oxygen is lower than measurements from Utiskuil et al. [29] data suggest, reflecting a known limitation of the EDC model under vitiated conditions to potentially over-predict reactivity of fuels. The average fuel mass fraction shows similar trends for all scenarios up to about 20 s. After that, there is a sharp increase in the gaseous fuel for the ventilated scenarios around 40 s as the crib ignites, with the less ventilated scenarios experiencing a similar increase except delayed due presumably to the lower temperatures in the cell delaying or retarding pyrolysis of the wood.

4. Discussion

Crib fire modeling involves a high number of complex behaviors, and consequently a large number of modeling studies are not found in the literature. Besides the complexity of some of the fundamental characterization including kinetics, properties, and multi-phase phenomenology, the degradation of the crib is a significant challenge as the crib experiences localized decomposition and ultimate collapse. As best as we can tell, this problem has not been addressed in prior studies. Model predictions are thought to be best in the early burn regime where the fire is still developing and the wood is still structurally representative of the initial crib build. To date, no modeling efforts have been found to capture the collapse feature of the burn, which is a behavior that would be needed for accurately predicting longer-term effects from crib burns.

In our scenario, we were not focused on the answer to the question of whether we can select properties that will produce a representative response. This differentiates our approach when compared with other prior efforts. Rather, we elected to select representative properties and tune one of the more sensitive properties, the heat of pyrolysis, for a representative crib burn rate under open conditions. As we transition to burning the crib in a partially closed scenario more representative of an urban burn scenario, the crib model tuned to the open conditions is anticipated to continue to burn in a representative way given the introduction of reduced oxygen via a decreasing opening size.

Our pyrolysis rate is principally governed by the thermal feedback from the environment, which in the open scenario included mostly the radiation and convection of the flames interacting with the solid. This simulation exercise focus was on whether present crib modeling methods would respond appropriately in an oxygen vitiated environment and exhibit appropriate extinction. This is a step towards being able to credibly predict large urban fire scenarios that are at present challenging to predict due to the scale of the physical domain. The enclosure scenarios largely followed the theoretically expected extinction behaviors as suggested by the ventilation parameter regimes previously identified. However, there is some uncertainty due to the lack of a definitive model behavior to target for assigning an extinction regime. Declining mass loss and declining compartment temperatures suggest both scenarios A and B are extinguishing (per Fig. 7A mass loss rate is 0.020 and 0.029 kg/s for case A and B, between 0.1 and 0.2 kg/s for cases C-E). This evidence suggests consistency with the historical findings from experimental characterization of ventilation parameters and provides promising evidence that the reaction modeling predictions are reasonably representative of physical behavior. Based on historical work, transitions between extinction regimes occur over a range of ventilation parameters around about $\Theta = 900$ g/m^{2}s. Our $\Theta = 600$ g/m^{2}s case A exhibited low mass loss from the crib (0.02 kg/s), with negligible soot emission (per Fig. 7B), average gas temperature below 400 compared to 600-900K for active burn scenarios, and low oxygen mass fraction (per Fig. 11D) A more detailed simulation study involving a more closely related set of test scenarios and multiple intervals per regime would be needed to demonstrate better reduction in uncertainty and better coordination between models and experiments. Our scenario was atypical of compartment fires where flashover is a key aspect. The scenarios did not include additional fuel sources to which fire may spread. In this respect, our work is more closely aligned with the fundamental extinction datasets than the compartment fire literature, both of which draw upon the ventilation parameter as a characteristic indicator.

A main benefit to having model predicting scenarios like this is the ability to more fully explore the response of the compartment to the scenario variations. We were able to evaluate properties difficult to determine from tests like the fraction of released energy resulting in heating of the walls, and integrated temperature, gaseous fuel, oxygen, and soot concentrations. These would be atypical measurements from testing in this type of environment, or difficult to obtain information. Wall heating due to a fire is seldom reported in test data, especially integrated over the domain. We find over 10% of the energy in the walls by 3 min for case E and D, with lower (6-7%) fractions for the cases closer to extinction. Integrated oxygen is also difficult to obtain, which we show diminishing to close to zero for the less ventilated cases (A and B, per Fig. 11 D). These are valuable features of the modeling because they expose additional components of the test environment and response. Accuracy of these assessments depends partially upon physical modeling and the verification and validation pedigree thereof. Uncertainty in these prediction-only products will depend on this, and perhaps to a greater extent on the propagation of assumed property and configuration uncertainties. These will contribute to varying extents to the ultimate prediction accuracy and can be addressed quantitatively by subsequent validation and model characterization efforts.

The crib models used here and cited in the prior studies are relatively new contributors to the scientific literature. Pyrolysis modeling like this has been done for a lot longer, but the ability to model the scales necessary to make the kinds of predictions being made now are still emerging and will likely be improving with time making possible simulations of larger-scale and more complex problems. As mentioned earlier, one of the current interests in crib fire models and studies, is their use for generating and benchmarking fire behavior models for use in large-scale wildfire simulations. The work in this study has particular use in this regard as the larger crib studies are more on par to the fuel loadings found in massive wildfire settings and the ventilation studies lend particularly well to the enclosed fire environments found in urban settings.

4.1. Implications for massive fire simulations

We have previously published on the uncertainties involved in modeling climate impacts of naturally-occurring massive fires [32] and there are recent recommendations by the US National Academy of Sciences [33] regarding the potential environmental effect of massive fires ignited by acts of war. Both activities suggest the importance of improving large-scale fire behavior models to help better address the enormous uncertainties surrounding the large-scale fire phenomena.

Massive fire simulators, particularly in urban settings, currently lack direct data for surrogate modeling. They are of such a scope that they are largely computational impossible to fully resolve flame-fuel dynamics while simultaneously resolving large fire-atmosphere feedback and phenomena. Massive urban fire simulations are becoming increasingly important to understand and characterize the impacts of natural-disaster wildfires (e.g. 2021 Marshall Colorado Fire, 2023 Lahaina Hawaii Fire, or 2024 Palisades California Fire) or the environmental effects of ignited fires from modern conventional or nuclear warfare, which has garnished recent increased interest and speculation with the world's evolving geopolitical state [34–38]. To understand and quantify the impacts of massive fire scenarios three important physical phenomena need to be captured: 1) the fire activity, 2) the atmospheric transport, and 3) the climate feedback. In the context of modern warfare, the second and third of these phenomena have been the subject of recent works [39–41], but limited work has been done on the fire activity under massive-fire scenarios. This current work can help to better capture it, especially, the fire as the heat and mass sources that drive subsequent atmospheric transport and climate feedback. This current work also provides important insights into fire spread in urban settings under large-scale fire scenarios, which is not well-understood: more accurately defined source terms will lead to improved characterization of fire spread mechanisms, such as thermal radiation and firebrand phenomenon, which is considered as the primary mechanism in historical large-scale urban fires [42].

To summarize large-scale fire activity into one phenomenon is an over-simplification of the process as fire activity should be broken down further to at least: the ignitions, particularly where multiple spatially and temporally-varied ignitions occur concurrent with secondary effects such as in the context of warfare; subsequent fire spread combined with fire-atmosphere interactions; particulate generation as a function of fuel loading and fire dynamics; and particulate lofting/fallout. This work can be used to better inform the latter two aspects of the fire activity phenomenon: particulate generation and lofting that are both fire dynamic (dependent on fire progression, fuel loading, and ventilation) and temporally variant instead of a one-time mass production/injection.

The results from the SIERRA/Fuego crib fire simulations can be combined with established crib fire scaling laws [6] to produce consumption rates of fuel, F (kg/s-m^2),

$$F = F' \left(\frac{L_F}{3.0}\right)^{1.25} \quad (2)$$

$$F' = \frac{0.315}{1 + e^{-3.78e-4(\Theta - 6136)}} \quad (3)$$

as a function of fuel loading (L_F) in kg/m^2 and the ventilation coefficient (Θ) described above. Derivation details for these equations are found in the supplementary material. To determine the rate of particulate emission, multiply F by an emission factor appropriate for the burning fuel and account for possible secondary burning which can occur outside the room and thus outside the simulations in this work. To determine the heat release rate of the fires multiply F by an appropriate heat of combustion for the burning fuel. These parameters, rates of particulate emission and heat release, could be integrated into a larger atmospheric transport model such as WRF [43], Higrad [44], or Fast-Eddy [45] to capture the mass and energy source terms of fire and smoke to better simulate massive fire impacts on large scales.

5. Conclusions

This multi-lab effort describes a relatively unique set of large-scale crib-fire tests with relevance to the large-scale fire problem. Modeling and simulation predictions are shown corresponding to the tests, with the mass loss of the open fire being equivalent to the data by modifying the heat of pyrolysis of the wood. The model utility is illustrated for approximating large-scale parameters for smoke lofting and transport. The crib fire is also modeled in a partial enclosure with varying ventilation. The extinction behavior of the model aligns reasonably well with extinction regimes based on the extinction parameter, suggesting the model incorporates sufficient physics to approximate vitiated burn conditions and crib response thereto. The work has implications for large-scale fire interrogation and represents progress towards the ability to address uncertainties in fire approximations needed to understand consequences of large-scale fires.

CRediT authorship contribution statement

Alexander L. Brown: Conceptualization, Formal analysis, Methodology, Software, Visualization, Writing – original draft, Writing – review & editing. **Sara McAllister:** Conceptualization, Data curation, Methodology, Supervision, Writing – original draft, Writing – review & editing. **Alexander J. Josephson:** Conceptualization, Methodology, Writing – original draft, Writing – review & editing. **Jon Reisner:** Conceptualization, Funding acquisition, Methodology, Supervision, Writing – review & editing. **Eunmo Koo:** Conceptualization, Methodology, Writing – original draft, Writing – review & editing.

Declaration of competing interest

The authors declare that they have no known competing financial interests or personal relationships that could have appeared to influence the work reported in this paper.

Acknowledgements

The baseline crib geometry and mesh were generated by Sol Alverio as part of a summer internship program. Sandia National Laboratories is a multi-mission laboratory managed and operated by National Technology & Engineering Solutions of Sandia, LLC (NTESS), a wholly owned subsidiary of Honeywell International Inc., for the U.S. Department of Energy's National Nuclear Security Administration (DOE/NNSA) under contract DE-NA0003525. This written work is authored by an employee of NTESS. The employee, not NTESS, owns the right, title and interest in and to the written work and is responsible for its contents. Any subjective views or opinions that might be expressed in the written work do not necessarily represent the views of the U.S. Government. The publisher acknowledges that the U.S. Government retains a non-exclusive, paid-up, irrevocable, world-wide license to publish or reproduce the published form of this written work or allow others to do so, for U.S. Government purposes. The DOE will provide public access to results of federally sponsored research in accordance with the DOE Public Access Plan. The experiments conducted by the USDA Forest Service at the-Missoula Fire Sciences Laboratory were supported by the National Fire Decision Support Center.

Appendix A. Supplementary data

Supplementary data to this article can be found online at https://doi.org/10.1016/j.firesaf.2026.104857.

References

[1] P.G. Smith, P.H. Thomas, The rate of burning of wood cribs, Fire Technol. 6 (1) (1970) 29–38.
[2] D. Gross, Experiments on the burning of cross piles of wood, J. Res. Nat. Burea Stand. Eng. Inst. 66c (2) (1962) 99–105.
[3] P.L. Blackshear J.R., A.M. Kanury, On the combustion of wood I: a scale effect in the pyrolysis of solids, Combust. Sci. Technol. 2 (1) (1970) 1–4.
[4] G. Heskestad, Modeling of enclosure fires, Symp. (Int.) Combust. 14 (1973) 1021–1030.
[5] M.A. Delichatsios, Fire growth rates in wood cribs, Combust. Flame 27 (1976) 267–278.
[6] R.I. Emori, K. Saito, A study of scaling laws in pool and crib fires, Combust. Sci. Technol. 31 (5–6) (1983) 217–231.
[7] B.K. Dhurandher, R. Kumar, A.K. Dhiman, A. Gupta, An impact of sudden ventilation in a compartment involving crib fire, Iranian J. Sci. Technol. Trans. Mech Eng 45 (2) (2021) 403–414.
[8] T.Z. Harmathy, Experimental study on the effect of ventilation on the burning of piles of solid fuels, Combust. Flame 31 (1978) 259–264.
[9] S. McAllister, M. Finney, Burning rates of wood cribs with implications for wildland fires, Fire Technol. 52 (6) (2016) 1755–1777.
[10] J.G. Quintiere, B.J. McCaffrey, The Burning of Wood and Plastic Cribs in an Enclosure, ume 1, National Bureau of Standards. NBSIR, Washington, D.C., 1980, pp. 80–205.
[11] N.P. Bryner, G.W. Mulholland, Smoke emission and burning rates for urban structures. Atmospheric environment. Part A, General Topics 25 (11) (1991) 2553–2562.
[12] T. Rappsilber, P. Below, S. Krüger, Wood crib fire tests to evaluate the influence of extinguishing media and jet type on extinguishing performance at close range, Fire Saf. J. 106 (2019) 136–145.
[13] R. Kallada Janardhan, S. Hostikka, Predictive computational fluid dynamics simulation of fire spread on wood cribs, Fire Technol. 55 (6) (2019) 2245–2268.
[14] Y. Xi, X. Dong, W. Chow, Numerical simulation on temperature in wood crib fires, Therm. Sci. 25 (4 Part A) (2021) 2621–2636.
[15] S. Zhang, X. Ni, M. Zhao, J. Feng, R. Zhang, Numerical simulation of wood crib fire behavior in a confined space using cone calorimeter data, J. Therm. Anal. Calorimetry 119 (3) (2015) 2291–2303.
[16] SIERRA Thermal/Fluid Development Team, "SIERRA Low Mach Module: Fuego Theory Manual," SAND2019-12289.
[17] Mendoza, H. Brown, A.L., Ricks, A., "Modeling high heat flux combustion of coniferous trees using chemically reacting lagrangian particles," for the Western States Section of the Combustion Institute Meeting, October 14-15, Albuquerque, NM, (SAND2019-10301C).
[18] Brown, A.L., Mendoza, H., Koo, E., Reisner, J., "A High Flux Forest Fire Scenario for Assessing Relative Model Accuracy for CFD Tools," for the Western States Section of the Combustion Institute Meeting, October 14-15, Albuquerque, NM, SAND2019-10541 C.
[19] K. Himoto, M. Shinohara, A. Sekizawa, K.I. Takanashi, H. Saiki, A field experiment on fire spread within a group of model houses, Fire Saf. J. 96 (2018) 105–114.
[20] F.A. Albini, J.K. Brown, R.D. Reinhardt Ed Ottmar, Calibration of a large fuel burnout model, Int. J. Wildland Fire 5 (1995) 173–192.
[21] I.-C. Ene, V. Iordache, M. Dima, I. Anghel, HRR-based calibration of an FDS model for office fire simulations using full-scale wood crib experiments, Appl. Sci. 15 (2025) 6909.
[22] J.A. Block, A theoretical and experimental study of nonpropagating free-burning fires, Symp. (Int.) Combust. 13 (1971) 971–978.
[23] S.R. Tieszen, S.P. Domino, A.R. Black, Validation of a Simple Turbulence Model Suitable for Closure of temporally-filtered Navier-Stokes Equations Using a Helium Plume, Sandia National Laboratories, June 2005. SAND2005-3210.

[24] B.F. Magnussen, B.H. Hjertager, On mathematical modeling of turbulent combustion with special emphasis on soot formation and combustion. 16th Symposium on Combustion, The Combustion Institute, 1977, pp. 719–729.
[25] B.F. Magnussen, On the structure of turbulence and a generalized eddy dissipation concept for chemical reactions in turbulent flow, in: 9th AIAA Sc. Meeting, St. Louis, MO, 1981. US.
[26] P.A. Tesner, T.D. Snegiriova, V.G. Knorre, Kinetics of dispersed carbon formation, Combust. Flame 17 (1971) 253–260.
[27] A.L. Brown, R.C. Shurtz, L.K. Takahashi, E.N. Coker, J.C. Hewson, M.L. Hobbs, Tritium Fires: Simulation and Safety Assessment, April 2022. SAND 2022-4187.
[28] Brown, A.L., J.C. Hewson, "Validating a fire simulation tool with a large-scale helium plume dataset," Paper TFEC-2022-40932, the 7th Thermal and Fluids Engineering Conference (TFEC) April - May, 2022, Partially Online Virtual and in Las Vegas, NV Conference SAND2022-1070 C.
[29] Y. Utiskul, J.G. Quintiere, A.S. Rangwala, B.A. Ringwelski, K. Wakatsuki, T. Naruse, Compartment fire phenomena under limited ventilation, Fire Saf. J. 40 (4) (2005) 367–390.
[30] J.L. Torero, A.H. Majdalani, C. Abecassis-Empis, A. Cowlard, Revisiting the compartment fire, Fire Saf. Sci. 11 (2014) 28–45.
[31] M.J. Antal, G. Várhegyi, E. Jakab, Cellulose pyrolysis kinetics: revisited, Ind. Eng. Chem. Res. 37 (4) (1998) 1267–1275.
[32] A.L. Brown, E. Koo, J. Reisner, Estimating stratospheric carbon from fires during a regional nuclear exchange, Fire Saf. J. 141 (2023) 103877.
[33] National Academies of Sciences, Engineering, and Medicine, Potential Environmental Effects of Nuclear War, The National Academies Press, Washington, DC, 2025, https://doi.org/10.17226/27515.
[34] A. Robock, Nuclear winter, WIREs Clim. Change 1 (3) (2010) 418–427.
[35] O.B. Toon, C.G. Bardeen, A. Robock, L. Xia, H. Kristensen, M. McKinzie, R. J. Peterson, C.S. Harrison, N.S. Lovenduski, R.P. Turco, Rapidly expanding nuclear arsenals in Pakistan and India portend regional and global catastrophe, Sci. Adv. 5 (10) (2019).
[36] A. Robock, L. Oman, G.L. Stenchikov, Nuclear winter revisited with a modern climate model and current nuclear arsenals: still catastrophic consequences, JGR: Atmospheres 112 (D13) (2007).
[37] J. Coupe, C.G. Bardeen, A. Robock, O.B. Toon, Nuclear winter responses to nuclear war between the United States and Russia in the whole atmosphere community climate model version 4 and the goddard institute for space Studies ModelE, JGR Atmospheres 124 (15) (2019) 8522–8543.
[38] J. Reisner, G. D'Angelo, E. Koo, W. Even, M. Hecht, E. Hunke, D. Comeau, R. Bos, J. Cooley, Climate impact of a regional nuclear weapons exchange: an improved assessment based on detailed source calculations, JGR Atmospheres 123 (5) (2018) 2752–2772.
[39] B.M. Wagman, K.A. Lundquist, Q. Tang, L.G. Glascoe, D.C. Bader, Examining the climate effects of a regional nuclear weapons exchange using a multiscale atmospheric modeling approach, JGR Atmospheres 125 (24) (2020) e2020JD033056.
[40] M.J. Mills, O.B. Toon, J. Lee-Taylor, A. Robock, Multidecadal global cooling and unprecedented ozone loss following a regional nuclear conflict, Earths Future 2 (4) (2014) 161–176.
[41] F.S.R. Pausata, J. Lindvall, A.M.L. Ekman, G. Svensson, Climate effects of a hypothetical regional nuclear war: sensitivity to emission duration and particle composition, Earths Future 4 (11) (2016) 498–511.
[42] E. Koo, P.J. Pagni, D.R. Weise, J.P. Woycheese, Firebrands and spotting ignition in large-scale fires, Int. J. Wildland Fire 19 (7) (2010) 818–843.
[43] W.C. Skamarock, et al., A description of the advanced research WRF version 4, NCAR Tech. Note NCAR/TN-556+STR (2019) 145.
[44] Kendra L. Van Buren, Jesse M. Canfield, François M. Hemez, Jeremy A. Sauer, Code Verification of the HIGRAD Computational Fluid Dynamics Model, Los Alamos National Laboratory, 2012. Technical Report, LA-UR-12-21165.
[45] J.A. Sauer, D. Muñoz-Esparza, The FastEddy® resident-GPU accelerated large-eddy simulation framework: model formulation, dynamical-core validation and performance benchmarks, J. Adv. Model. Earth Syst. 12 (2020) e2020MS002100.